

IFUSP/P-736  
B.I.F. - USP

UNIVERSIDADE DE SÃO PAULO

# PUBLICAÇÕES

INSTITUTO DE FÍSICA  
CAIXA POSTAL 20516  
01498 - SÃO PAULO - SP  
BRASIL

IFUSP/P-736

13 JAN 1989



DISRUPTIVE INSTABILITIES IN THE DISCHARGES OF  
THE TBR-1 SMALL TOKAMAK

A. Vannucci, I.C. Nascimento, I.L. Caldas  
Instituto de Física, Universidade de São Paulo

Setembro/1988

DISRUPTIVE INSTABILITIES IN THE DISCHARGES OF THE TBR-1  
SMALL TOKAMAK \*

A. Vannucci, I.C. Nascimento, I.L. Caldas<sup>†</sup>  
Instituto de Física, Universidade de Sao Paulo  
C.P. 20.516, 01498 -- Sao Paulo - SP, Brazil

Abstract: Minor and major disruptions as well sawteeth oscillations (internal disruptions) were identified in the discharges of the small tokamak TBR-1, and their main characteristics investigated. The coupling of a growing  $m=2$  resistive mode with a  $m=1$  perturbation seems to be the basic process for the development of a major disruption, while the minor disruption could be associated to the growing of a stochastic region of the plasma between the  $q=2$  and  $q=3$  islands. Measured sawteeth periods were compared with the ones predicted by scaling laws and good agreement was reached. The time necessary for the sawteeth crashes also agrees with the values expected from the Kadomtsev's model. However, there are some sawteeth oscillations, corresponding to conditions of high  $Z_{eff}$  of the plasma, which showed longer crashes and could not be explained by this model.

I - INTRODUCTION

Energy dissipation and the complete loss of confinement of the plasma are the most harmful characteristics of the disruptive instabilities, which are usually classified as internal (sawteeth) and external (minor and major), accordingly to their global features. In spite of the intensive efforts expended since the last

<sup>†</sup>to be published in Plasma Physics and Controlled Fusion

decade the exact comprehension of the mechanisms that lead to any one of these disruptions are far to be well understood.

The sawteeth oscillations after been discovered by Von Goeler et al. (VON GOELER et al., 1974) were, in many aspects, explained by the Kadomtsev's model (KADOMTSEV, 1975), which was further supported by numerical simulations (WADELL et al., 1976; SYKES and WESSON, 1976) and even by experimental observations (JAHNS et al., 1978). Later on several experimental evidences were pointed out which did not supported this model anymore. They involved, for example, the detection of internal disruptions without any precursor oscillation and the  $m/n=1/1$  mode only after the sawtooth crash (CAMPBELL et al., 1986), the appearance of "giant" and "monster" sawteeth (PFEIFER, 1985; CAMPBELL et al., 1987) and, more recently, the evidence that  $q(0)$  keeps bellow unity all through the sawtooth phenomenon (WEST et al., 1987). Although alternative theories were formulated (DUBOIS et al., 1983; WESSON, 1986), the exact phenomenological mechanism that leads to an internal disruption is not completely known.

The external disruptive instabilities, called minor and major disruptions depending on the intensity they disturb the plasma column (MIRNOV, 1979), had been also intensively investigated. Negative spikes in the loop voltage signal, rapid losses of confined energy, sudden expansion of the minor radius with a diminution of the major radius are their main characteristics. It is furthermore typically verified an intense MHD activity with a frequency decrease and a fast (sometimes explosive) growth in amplitude, associated with an external disruption occurrence.

The major disruption, since it naturally leads to the complete destruction of the plasma confinement, is the one which deserves more attention. The knowledge of the processes through which a major disruption is created (so

controlling mechanisms could be therefore developed) is very important for the reliability of the future fusion reactors.

Several explanations were already proposed to clarify the external disruption occurrence; almost all of them involving the  $m/n=2/1$  amplitude increase as the main responsible for the disruption. The interaction of the  $q=2$  islands with the limiter, the coupling between the  $m/n=2/1$  and  $m/n=1/1$  modes (KARGER et al., 1976) and the destabilization of odd  $m$ -values modes as  $m/n=3/2, 5/3$ , etc. by the growing  $q=2$  islands (WADDEL et al., 1978) are some of the mechanisms more accepted for a major disruption development. The minor disruption, on the other hand, could be explained considering the existence of secondary magnetic islands between the principal islands. The superposition of these small islands would create an ergodic region inside the plasma. As the perturbation grows the ergodic region becomes larger until the whole system is affected and the collapse is characterized (FINN, 1975; RECHESLER and STIX, 1976).

Experimental evidences were already reported supporting each one of these models. While the presence of  $m/n=2/1, 3/2$  and  $5/3$  modes were detected right before a major disruption event (McGUIRE and ROBINSON, 1980), in other experiments the interaction of  $q=2$  islands with the limiter (ROBERTS et al., 1986) and the  $m/n=2/1$  and  $1/1$  modes coupling (EQUIPE TFR, 1977) were clearly identified. On the other hand, it was also observed that the perturbation which leads to a major disruption begins between the  $q=1$  and  $q=2$  magnetic surfaces (HUTCHINSON, 1976); this would therefore be favourable to the magnetic lines braiding model.

Since the present knowledge about the disruptive phenomena is still inconclusive in many aspects, it seems that any further contribution to this "status-quo" should be welcome. Considering this point of view the plasma disruptions in the small size and low  $\beta$  TBR-1 discharges were therefore investigated and reported here.

## II - EXPERIMENTAL SET UP AND MEASUREMENTS

The TBR-1 basic parameters are:  $R_0=0.30\text{m}$ ,  $a=0.08\text{m}$ ,  $B_0 \sim 0.4\text{T}$ ,  $T_0 \sim 200\text{eV}$ ,  $6 \leq I_p \leq 12\text{kA}$  and discharge duration ranging up to 7ms. The two main diagnostics used in this work were a soft x-ray detection system and a set of 20 Mirnov coils. The soft x-ray flux from the plasma was measured by an array of six surface-barrier detectors (ORTEC model CR 019-50-100) placed inside an imaging camera. Each detector viewed a different plasma volume through a solid angle delimited by a polypropylene covered slot. The output signals, after being properly amplified, were digitalized and recorded through a PC-microcomputer.

The poloidal magnetic field perturbation was measured by 16 pick-up coils equally spaced in the poloidal direction and 4 in the toroidal direction. All these coils were positioned inside the toroidal camera to avoid field attenuation by the wall of the vessel (TAN et al., 1986).

In respect to each type of disruption investigated, internal and external (minor and major), the obtained experimental results will now be presented and analysed separately.

### i) Internal disruption

Operating the TBR-1 device with high plasma current ( $I_p \sim 12\text{kA}$ ) and  $3.0 \leq q(a) \leq 3.5$ , the presence of sawteeth events were identified in  $\leq 10\%$  of the discharges. A typical example is shown in fig. 1b. The period and amplitude of the sawteeth are seen to change slightly with time. The average frequency is about 7.5kHz and no transients are verified in the loop voltage signal (fig. 1c)

during the sawteeth activity. It was also observed that they show the expected  $m=1$  oscillation superimposed to them.

Temporal expansion of soft x-ray and magnetic pick-up coil signals of this discharge are shown in fig. 2. Inverted sawtooth is observed (fig. 2b) for each sawtooth crash (fig. 2a). Observing, furthermore, the pick-up coils signals it is usually seen a fast increase in amplitude of the perturbed poloidal magnetic field associated with the sawteeth crashes (fig. 2c). This would be related to the energy transport from the inner to the outer region of the  $q=1$  magnetic surface.

In respect to the superimposed  $m/n=1/1$  oscillations it was indeed verified, many times, that their amplitudes showed a growing behaviour just before the sawteeth crashes. This could suggest that the  $q=1$  growing magnetic island would be responsible for the internal disruptions development through the reconnective field lines model. However, it was more often observed examples in which the amplitude did not exhibit any grow at all. In some occasions even an intensity decrease was verified. These aspects are well exemplified in fig. 3 where some sawteeth events from three different discharges were grouped. The average growth rate of the oscillations assinalled by (\*) is  $2.6 \times 10^4 \text{ s}^{-1}$ .

Another interesting experimental feature is related to the observation of a sawtooth relaxation, occurring always more to the end of the discharges. This was usually accompanied by a stronger and saturated MHD activity. In fig. 4, where the central soft x-ray and perturbed magnetic field signals are temporally expanded, this aspect can be better evaluated.

The average time for the sawteeth crashes, in several discharges, was measured in the interval  $13 \mu\text{s} \leq \tau_c \leq 26 \mu\text{s}$ . However, when the sawteeth were preceeded by minor disruptions, which deteriorated the confinement and increased the plasma's  $Z_{\text{eff}}$ , the crashes did not show

anymore a rapid and sharp decay as in figs. 3a and 3b. Now, the decay times almost triplicate and  $m/n=1/1$  oscillations were detected during all their way down (fig. 3c).

Concerning the sawteeth periods the experimental values obtained ranged from  $100 \mu\text{s}$  to  $170 \mu\text{s}$ . It was not noticed any influence of the plasma's  $Z_{\text{eff}}$  conditions over this parameter.

#### ii) Minor disruption

This type of disruptive instability was very commonly observed in TBR-1 tokamak. In fig. 5, a sequence of minor disruptions are observed all along the discharge. The negative spikes in the loop voltage show the exact instants each disruption took place. The slow rises and fast decays in the soft x-ray signals (fig. 5c) are similar and simultaneous for all detectors. The MHD activity (fig. 5e) exhibit a fast growth in amplitude prior to the negative spikes (fig. 5d). The plasma current and column position exhibit also slight discontinuities in their signals (figs. 5a and 5b, respectively), suggesting a rather agitated and unstable plasma.

Different initial fields adjustments lead to other equilibrium conditions which make the discharges to be usually longer and minor disruptions are therefore identified only at the beginning. In fig. 6, for example, it is shown a discharge in which minor disruptions are followed by sawteeth fluctuations.

Fourier analysis indicated that the dominant  $m/n=2/1$  and  $3/1$  modes are the dominant precursor modes associated with the minor disruptions. The average MHD growth rate was  $5 \times 10^4 \text{ s}^{-1}$  and  $\bar{E}_\theta/B_\theta \sim 2\%$ , typically.

Taking the measured perturbation amplitude, corresponding to the  $m=2$  and  $m=3$  modes of a particular minor disruption event, and calculating the locations and half-

widths of the magnetic islands, the corresponding stochasticity parameter  $S$  clearly indicated an overlapping between them. The associated Poincare maps for the field lines distribution were obtained by integrating the magnetic field line equations determined somewhere (FERNANDES et al., 1988). The resulting diagrams for two different times, 50  $\mu$ s before and at the exact instant of the negative spike appearance in the loop voltage, are shown in figs. 7a and 7b, respectively. In this example the disruption took place while the plasma column was centered.

### iii) Major disruption

The major disruptions in TBR-1 discharges with  $3.0 \leq q(a) \leq 4.0$  are usually characterized by a noticeable growing precursor activity, a negative spike in the loop voltage signal and a small displacement of the plasma column towards the inner part of the torus. Typical duration of the major disruptive events detected was  $\tau_D \sim 200 \mu$ s.

The perturbed poloidal field ratio, right before the appearance of the negative spike was  $\bar{B}_\theta/B_\theta \sim 4\%$  and the precursor oscillation growth rate ranged from  $1.4 \times 10^3 \text{s}^{-1}$  to  $8.9 \times 10^4 \text{s}^{-1}$ . Fourier analysing the MHD signals it was observed that the  $m/n=2/1$  was always the dominant and responsible mode for the major disruptions observed.

Calculations made about the  $q=2$  resonant magnetic surface localization and the half-width of its corresponding islands (FERNANDES et al., 1988) showed that there was no possibility of an island-limiter interaction. On the other hand, the  $m/n=2/1$  and  $1/1$  modes coupling could be a realistic mechanism through which the disruption would occur. This interpretation is based upon the observation of the soft x-ray and MHD signals in figs. 8a and 8b, respectively. The frequencies of these two modes change and

finally assume the same values right before the negative spike occurrence in the loop voltage (fig. 8c), indicating an interaction between them.

In other discharges again the  $m/n=1/1$  and  $2/1$  assume the same frequencies before a major disruption, as it is shown in fig. 9, but now there is no amplitude growth of the  $m/n=1/1$  mode (fig. 9b). This behaviour strengthens the idea that the  $q=2$  islands are, in fact, the greatest responsible for the major disruptions.

Another interesting aspect concerning some TBR-1 discharges is the interaction between the plasma column and the wall (or limiter) of the vessel, due to the lack of feed-back control. If the plasma column moves towards the inner part of the toroidal chamber, the interaction simply annihilated the confinement. The time-lag between the interaction and the complete destruction of the plasma is in average about 100  $\mu$ s. This value is one half of the plasma destruction time in a major disruption, indicating that the former is even a more violent phenomenon than the latter. The absence of negative spikes in the loop voltage and a lack of MHD growing modes prior to the plasma-limiter interaction are other observed characteristics that configurate this type of discharge ending.

On the other hand, when the interaction happens in the outer side of the vessel, the confinement is not lost. A fast plasma cooling is verified through the soft x-ray emission and the loop voltage is strongly affected by the event. Afterwards, it is usually observed an increase of the plasma temperature accompanied by strong  $m/n=1/1$  oscillations or even sawteeth fluctuations.

### III - DISCUSSION AND CONCLUSIONS

The data presented in this paper shows that even a small scale device like the TBR-1 exhibits similar

behaviour to larger sizes tokamaks, concerning the disruptive instabilities.

The experimental values obtained for the sawteeth periods (100  $\mu$ s to 170  $\mu$ s) were compared with the ones expected from scaling laws. Reasonable agreement was achieved by using the expressions from (McGUIRE and ROBINSON, 1979) and (KADOMTSEV, 1984) which gave 87  $\mu$ s and 210  $\mu$ s, respectively.

The previously mentioned sawteeth relaxation is an interesting phenomenon which has been also observed somewhere (EQUIPE TFR, 1977). The explanation proposed based upon the existence of two  $m/n=1/1$  modes with different frequencies, one of them being the direct responsible for the internal disruptions, could not be confirmed in this work.

The predicted sawtooth crash-time from Kadomtsev's model using the TBR-1 parameters, was estimated to be  $\tau_c \sim 18 \mu$ s. This value is comparable to the measured ones in normal discharges, where  $13 \mu$ s  $\leq \tau_c \leq 26 \mu$ s. The values obtained on high  $Z_{eff}$  discharges, on the other hand, are too larger to be explained by this model. Furthermore, the observation of internal disruptions without the growing  $m/n=1/1$  precursor oscillation is another indication that the reconnective model is not fully appropriated to describe the sawtooth instability and new explanations have to be formulated for a complete understanding of this phenomenon.

When the plasma is well formed and the column centered, it was verified that the minor disruptions in TBR-1 could be explained in terms of a superposition of the  $m=2$  and  $m=3$  MHD modes. The amplitude of the poloidal magnetic field perturbation, as was mentioned before, is  $\bar{B}_\theta/B_0 \sim 2\%$ , typically.

The construction of Poincare maps 50  $\mu$ s before and at the instant of the disruption, figs. 7a and 7b, well illustrates the ergodization of the magnetic field lines between the principal islands. Near the magnetic axis a

circle-like closed line pattern is formed. Outwards, near the magnetic islands, the intersecting points do not form a closed line anymore. They are displaced almost randomly and this effect is stronger for higher amplitude perturbations. Comparing the pictures in figs. 7a and 7b it is verified that the islands shrink and the chaotic region increases as the perturbation amplitude grows. The destruction of magnetic surfaces seems to trigger the observed minor disruptions. This behaviour is consistent with the theory proposed by Finn (FINN, 1975) and others (RECHESTER and STIX, 1976).

Finally, it was observed that the mode coupling between  $m/n=1/1$  and  $m/n=2/1$  modes would be the responsible mechanism through which a major disruption would be developed. This was concluded because these two modes exhibit the same frequency just before the disruption event. The associated poloidal field ratio is  $\bar{B}_\theta/B_0 \sim 4\%$ .

Calculations done over the localizations and half-widths of the magnetic islands showed that any interaction between the islands and the limiter can be discarded. No evidence of the  $m/n=3/2$  mode predicted in some theories (WADDELL et al., 1978) was, in the same way, found prior the major disruptions.

ACKNOWLEDGEMENT: The authors would like to thank Dr. M.V.A.P. Heller for the computer code in the Poincare maps construction.

<sup>†</sup>Partially supported by CNPq

## REFERENCES

- CAMPBELL D.J. et al. (1986) Nucl. Fus. 26, 1085.
- CAMPBELL D.J. et al. (1987) in the 11<sup>th</sup> Int. Conf. Plasma Phys. Contr. Fus. Res., Kyoto, IAEA-CN-47/A-VII-5, 433.
- DUBOIS M.A., PECQUET A.L. and REVERDIN C. (1983) Nucl. Fus. 23, 147.
- EQUIPE TFR (1977) Nucl. Fus. 17, 1283.
- FERNANDES A.S., HELLER M.V.A.P., CALDAS I.L. (1988) Plasma Phys. Contr. Fusion, to be published.
- FINN J.M. (1975 Nucl. Fus. 15, 845.
- HUTCHINSON I.H. (1976) Phys. Rev. Lett. 37, 338.
- JAHNS G.L. et al. (1978) Nucl. Fus. 18, 609.
- KADOMTSEV B.B. (1975) Sov. J. Plasma Phys. 1, 389.
- KADOMTSEV B.B. (1984) Plasma Phys. Contr. Fusion 26, 217.
- KARGER F. et al. (1976) in 6th Int. Conf. Plasma Phys. Contr. Fus. Res., Berchtesgaden, IAEA-CN-35/A-7.
- McGUIRE K., ROBINSON D.C. (1980) Phys. Rev. Lett. 44, 1666.
- MIRNOV S.V. (1979) in IAEA Symposium on Current Disruptions in Toroidal Devices, Garching, B-1.
- RECHESTER A. B., STIX T.H. (1976) Phys. Rev. Lett. 36, 587.
- ROBERTS D.E. et al. (1986) Nucl. Fus. 26, 785.
- SYKES A. and WESSON J.A. (1976) Phys. Rev. Lett. 37, 140
- TAN I.H. et al. (1986) IEEE Trans. Plasma Sci. PS-14, 279.
- VON GOELER S. et al. (1974) Phys. Rev. Lett. 33, 1201.
- WADDELL B.V. et al. (1976) Nucl. Fus. 16, 528.
- WADDELL B.V. et al. (1978) Phys. Rev. Lett. 41, 1386.
- WESSON J.A. (1986) Plasma Phys. Contr. Fusion 28, 243.
- WEST W.P. et al. (1987) Phys. Rev. Lett. 58, 2758.

## FIGURE CAPTIONS

- FIG. 1 - Plasma current (a), soft x-ray signal (central chord) showing sawteeth oscillations (b) and loop voltage (c) in a typical TBR-1 discharge.
- FIG. 2 - X-rays and MHD activity signals in expanded time scale corresponding to the discharge shown in fig. 1. No increase in the MHD activity prior to each sawtooth crash is observed.
- FIG. 3 - Examples of sawteeth fluctuation from three different discharges. The  $m/n=1/1$  oscillation amplitude does not always increase in a sawtooth period. The crashes are longer for discharges with high  $Z_{\text{eff}}$  condition (c). The events assinalled by (\*) had their growth rate measured to be  $2.6 \times 10^4 \text{ s}^{-1}$  average.
- FIG. 4 - Soft x-ray (a) and MHD activity (b) temporal evolution. The arrow indicates the beginning of the sawteeth relaxation giving place to a strong  $m/n=1/1$  oscillation, accompanied by a saturated MHD oscillation.
- FIG. 5 - Plasma current (a), horizontal position (b), soft x-ray emission (c), loop voltage (d) and MHD activity (e) evolution during a discharge in which successive minor disruptions occurred.
- FIG. 6 - Minor disruptions are initially observed but afterwards the equilibrium conditions change and sawteeth fluctuations are then identified.
- FIG. 7 - Intersection of magnetic field lines with a poloidal plane  $50 \mu\text{s}$  before (a) and at the instant (b) of a minor disruption occurrence. The islands shrink as the chaotic region between them increases.
- FIG. 8 - The  $m/n=1/1$  oscillation in soft x-ray signal (a) and the  $m/n=2/1$  dominant MHD mode (b) have the same frequency just prior a major disruption indicating mode coupling.
- FIG. 9 - The  $m/n=1/1$  and  $2/1$  mode coupling is again identified (b and c) but now the  $m/n=1/1$  oscillation amplitude does not increase anymore before the major disruption (a and b).

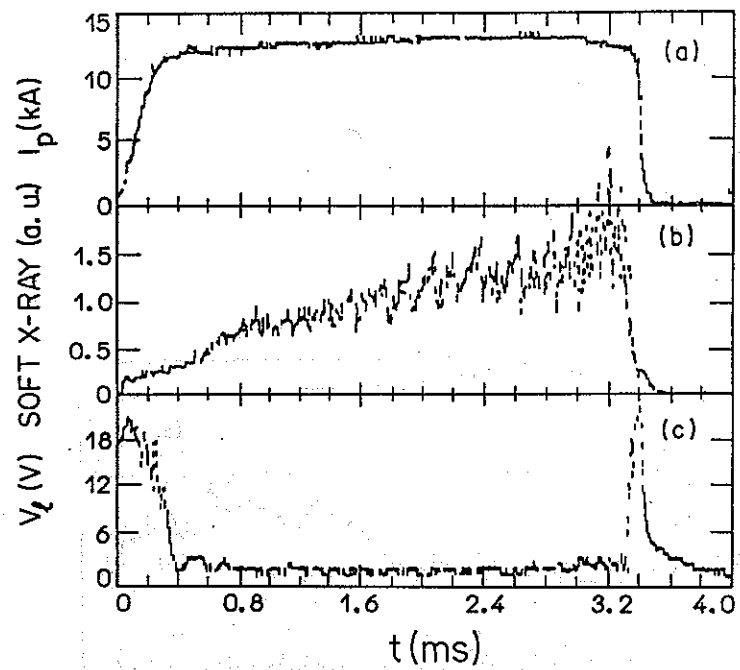


fig. 1

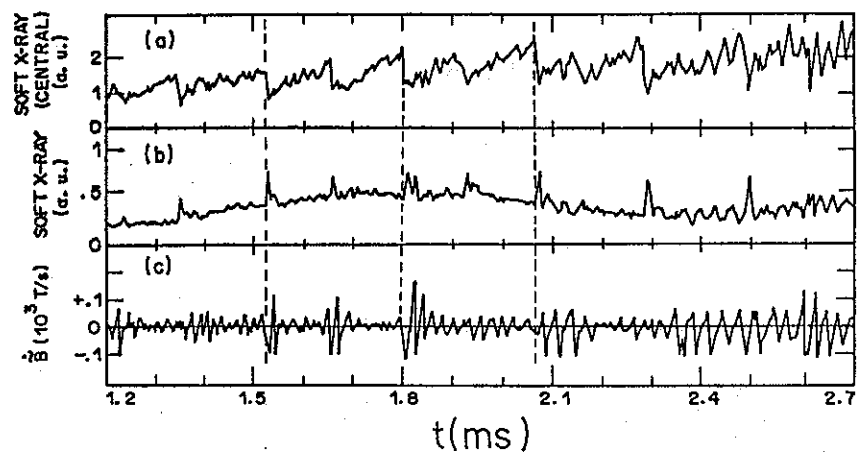


fig. 2

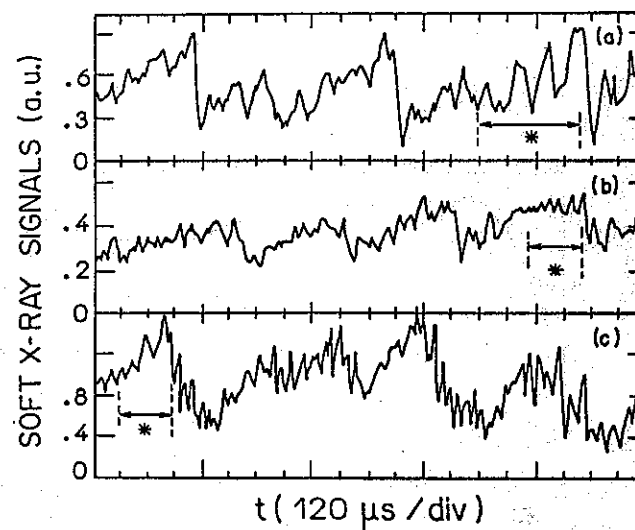


fig. 3

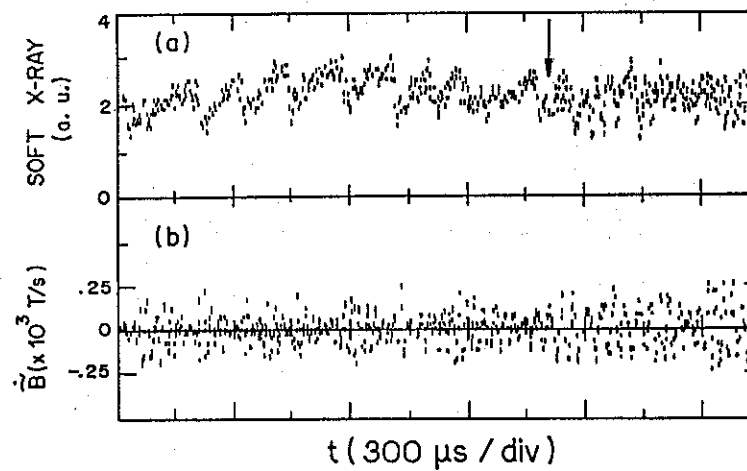


fig. 4



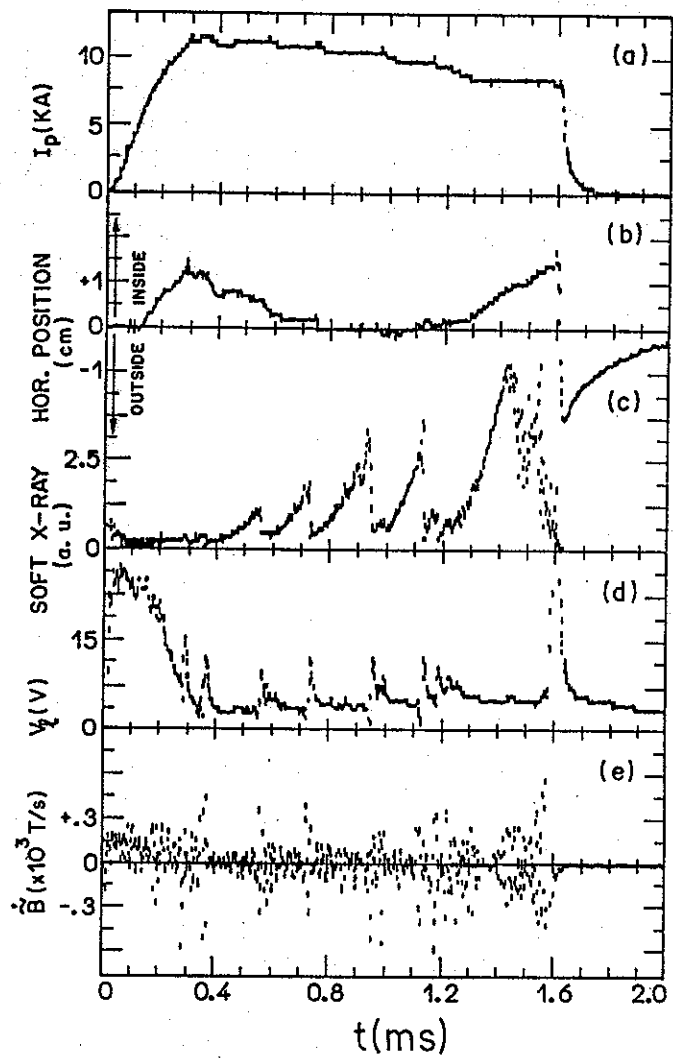


fig. 5

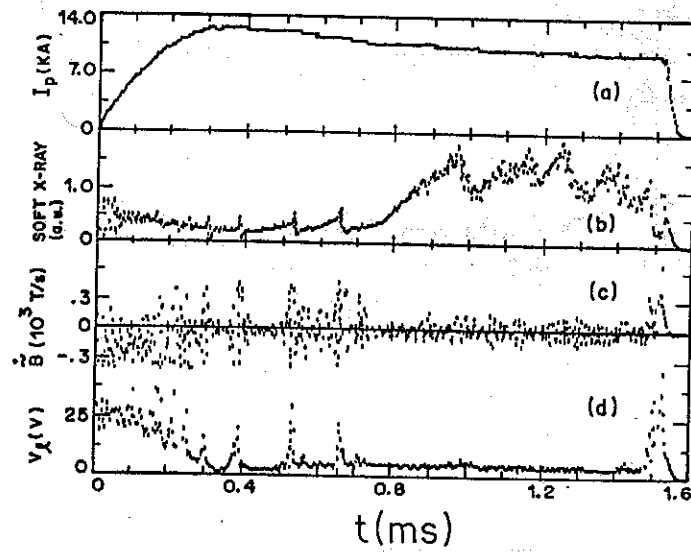


fig. 6

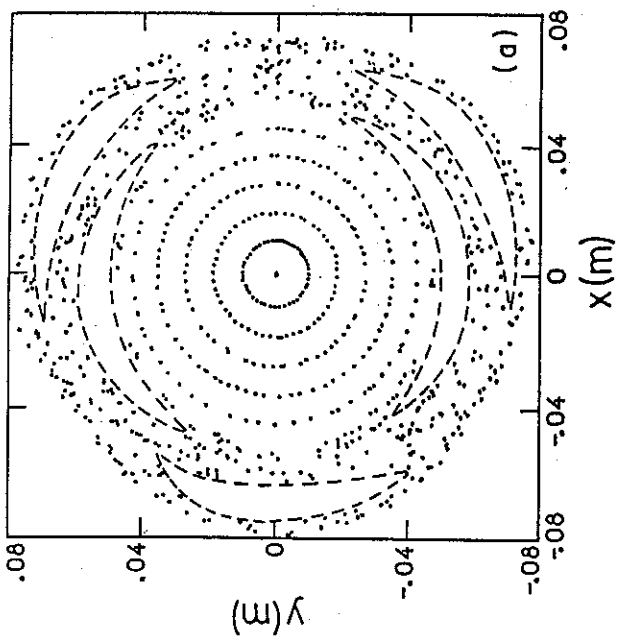
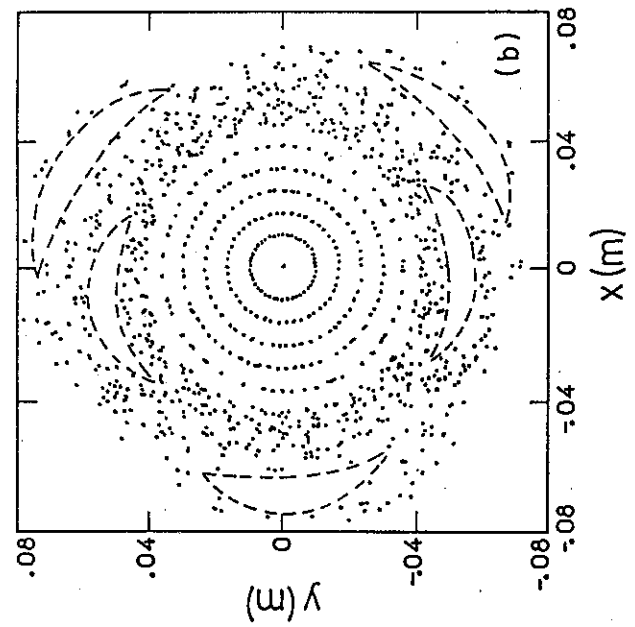


fig. 7

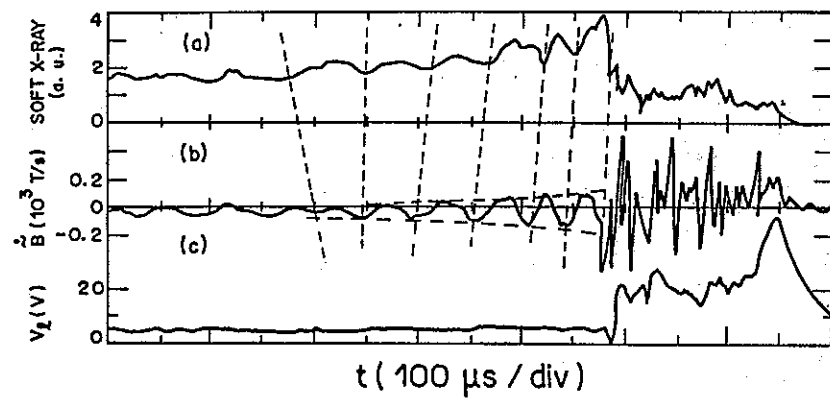


fig. 8

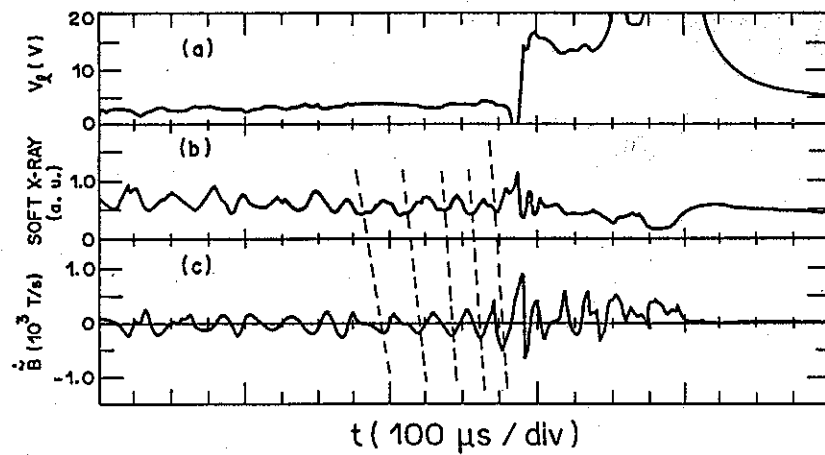


fig. 9